American Mineralogist, Volume 89, pages 1701–1708, 2004

High-pressure viscometry of polymerized silicate melts and limitations of the Eyring equation

DAVID TINKER,[1,*] CHARLES E. LESHER,[1] GREGORY M. BAXTER,[1] TAKEYUKI UCHIDA,[2] AND YANBIN WANG[2]

[1]Department of Geology, University of California, One Shields Avenue, Davis, California 95616, U.S.A.
[2]Consortium for Advanced Radiation Sources, University of Chicago, Chicago, Illinois 60637, U.S.A.

ABSTRACT

In situ falling-sphere measurements of viscosity have been performed to determine the viscosity of dacite melt (68 wt% SiO_2) from 1.5 to 7.1 GPa at temperatures between 1730 and 1950 K, using the T-25 MA8 multianvil apparatus at the GSECARS 13-ID-D beamline at the Advanced Photon Source, Argonne National Lab. The viscosity of dacite melt decreases between 1.5 and 7.1 GPa. At 1.5 GPa and 1825 K the viscosity is 86.6 ± 17.3 Pa·s, whereas at 6.6 GPa and 1900 K it is 2.8 ± 0.6 Pa·s. The negative pressure dependence of viscosity results in an activation volume of –12.4 ± 1.4 cm^3/mol at 1800 K and –5.1 ± 0.9 cm^3/mol at 1900 K. These new data are compared with viscosities estimated from the Eyring equation using oxygen self-diffusion data for the same bulk composition at high pressures. The Eyring equation generally predicts viscosities that are greater than measured viscosities. In addition, the Eyring equation predicts a minimum viscosity at 5 GPa, but no minimum was seen in our falling sphere data set. These discrepancies suggest that the mechanisms for viscous flow and self-diffusion of oxygen in polymerized melts may differ at high pressures, thus limiting the utility of the Eyring equation for high-pressure extrapolations. Further development of the Adam-Gibbs theory may provide an alternative for relating self-diffusion and viscosity at high pressures.

INTRODUCTION

Understanding the transport properties of silicate melts at high pressures is critical for modeling igneous processes in the Earth's mantle. Two methods commonly have been employed to determine melt viscosity at mantle pressures. Traditionally, a high-density sphere is placed at the top of a sample chamber where it may settle through the sample once the sample melts. The settling velocity of the sphere is determined from the difference between the initial and final positions of the sphere and elapsed settling time. Stokes' Law is then solved for viscosity, knowing the sphere radius, settling velocity, and the sphere-melt density contrast, and correcting for wall effects in the sample chamber. Falling-sphere measurements of viscosity in quench experiments (hereafter fall-and-quench experiments) largely have been limited to pressures below 2.5 GPa using the piston cylinder device (e.g., Kushiro 1976, 1978), although the technique has been extended to 7 GPa using a multianvil apparatus (Mori et al. 2000). More commonly, at pressures greater than 2.5 GPa, melt viscosity is estimated from the Eyring relationship, using measured or extrapolated oxygen (O) self-diffusion data and assuming a diffusion jump distance of 2.8 Å (e.g., Rubie et al. 1993). However, the validity of the Eyring relationship must be critically evaluated for silicate melts that exhibit maximum (Poe et al. 1997; Tinker and Lesher 2001) or minimum (Reid et al. 2001) O self-diffusion coefficients at elevated pressures.

Experimental efforts to measure melt viscosities directly at high pressures have been advanced greatly in recent years by the installation of large-volume multianvil devices at synchrotron X-ray facilities (e.g., Kanzaki et al. 1987; Rivers et al. 1998). Real-time X-ray radiography offers the opportunity to continuously monitor the motion of an X-ray-opaque marker sphere during its descent (or ascent) through a melt. This capability eliminates many of the problems of accurately determining time-distance relationships in fall-and-quench experiments. Synchrotron X-ray-based experiments have the additional advantage that experimental pressure can be determined by X-ray diffraction of a pressure standard placed within the pressure cell. This technique has been applied to Fe and Fe-sulfide liquids (e.g., Rutter et al. 2002; Secco et al. 2002), and albite (Suzuki et al. 2002; Kanzaki et al. 1987) and diopside (Reid et al. 2003) silicate melts. Viscosities determined in the latter studies are generally consistent with those from fall-and-quench experiments (Kushiro 1976, 1978; Mori et al. 2000, among others).

Previous studies have focused on the relationship between melt polymerization and the pressure dependence of melt viscosity. Kushiro (1976) found that the viscosity of fully polymerized $NaAlSi_2O_6$ (jadeite) melt decreased by nearly an order of magnitude between 0.5 and 2.4 GPa (i.e., the viscosity showed a negative pressure dependence). Kushiro (1978) reported a similar decrease in the viscosity of fully polymerized $NaAlSi_3O_8$ (albite) melt between 1 atm and 2 GPa. Mori et al. (2000) extended the study of albite melt using the fall-and-quench method in the multianvil apparatus, and found a negative pressure dependence from 3 to 7 GPa that was similar to that reported by Kushiro (1978). In contrast, Scarfe et al. (1987) measured the viscosity of depolymerized $CaMgSi_2O_6$ (diopside) melt, and found that melt viscosity increased by a factor of four between atmospheric pressure and 1.5 GPa at 1913 K (i.e., the viscosity showed a positive pressure dependence). Scarfe et al. provided a nice summary of earlier measurements of melt viscosity and showed that the magnitude of the pressure effect on melt vis-

* E-mail: Tinker@geology.ucdavis.edu

cosity is a function of polymerization. Generally, proportional changes in the viscosities of depolymerized melts are greater than those for polymerized melts. Interestingly, the viscosities of some melt compositions exhibit changes in the sign of pressure dependence. For example, Brearley et al. (1986) found that the viscosity of partially polymerized $Ab_{25}Di_{75}$ (mol%) passes through a minimum at 1.2 GPa.

The main goal of the present study is to determine the pressure dependence of the viscosity of dacite (68 wt% SiO_2) melt. This composition is ideal for study because it is a naturally occurring silicic composition that we used in a study of Si and O self-diffusion (Tinker and Lesher 2001). In that earlier study, we concluded that Si and O self-diffusion occurs by the formation of high-coordinated Si and Al, similar to the mechanism in basalt melt (Lesher et al. 1996). This similarity shows that the mechanisms for melt transport at high pressures may be the same for partially to relatively polymerized melt compositions, so the dacite composition is a close analog for polymerized melts potentially formed by low-degree melting of peridotites (or eclogites) at high pressures (Baker et al. 1995). Experimentally, silicic compositions offer the advantages of attainable melting temperatures at high pressures and the expected high viscosities should lead to easily interpreted falling-sphere results (i.e., low velocities of falling spheres). From a theoretical perspective, measured viscosities of dacite melt at high pressures are useful because they allow a direct comparison with O self-diffusion results in our earlier study (Tinker and Lesher 2001).

We have characterized high-pressure dacite melt viscosity using real-time falling sphere measurements. We use the results of these measurements to evaluate the Eyring equation and to gain insights into mechanisms for viscous flow and O self-diffusion in silicate melts at mantle conditions.

Experimental methods

The starting material for these experiments was synthesized from laboratory reagents (Fisher Scientific, Inc.) (Table 1). The powder mixture was fused at 1723 K and one atmosphere of N_2 for 30 minutes and quenched to glass. The recovered glass was ground to a <25 μm powder in a mortar and pestle. This process was repeated four times to ensure homogeneity of the starting material. The composition of the starting material is given in Table 1, where it is compared to the starting material used in our earlier study of Si and O self-diffusion (Tinker and Lesher 2001).

For each experiment, the starting material was packed firmly into a 1.8 mm I.D. × 1.5 mm long graphite cylinder with a platinum (Pt) sphere (90–300 μm in diameter) placed just below the top surface of the cylinder and covered with a thin layer of sample powder to prevent initial contact with the upper Pt lid. Following Hazen and Sharpe (1983), Pt spheres were formed by explosively melting 0.1 and 0.025 mm diameter Pt wire using an arc welder. The ends of the graphite cylinders were capped by Pt discs to provide X-ray-opaque reference markers during each experiment (see Figs. 1 and 2). The capsule was insulated from the sectioned graphite furnace by a sleeve of crushable alumina (An900). A 0.7 mm thick disc of MgO and BN powder (4:1 by weight) was placed directly above the sample capsule as a pressure standard. The top of the pressure standard was marked by a third Pt disc also forming the junction for the positive and negative leads of the W-3% Re vs. W-25% Re (D-type) thermocouple. No correction was made for the effect of pressure on thermocouple emf. The surrounding pressure medium was composed of Ceramacast 584-OF cast to fit WC anvils with truncation edge length (TEL) of 10 mm (Walker 1991). Experimental assemblies were stored under vacuum at 383 K until used.

We conducted in situ falling-sphere experiments from 1.5 to 7.1 GPa at temperatures between 1730 and 1950 K, using the T-25 MA8 multianvil apparatus in the 1000 ton press frame on the GSECARS 13-ID-D beamline at the Advanced Photon Source (APS), Argonne National Lab (Rivers et al. 1998) (Table 2). Uchida et al. (2002) described the physical configuration of the T-25. In the experimental hutch, the position of the X-ray beam is fixed and the press frame is mounted on a motorized table with five degrees of freedom and positioning accuracy within 0.1 mm. This "goniometer" allows precise centering of the sample to optimize X-ray diffraction and radiography, as described by Uchida et al. (2001). In the diffraction mode, the incident and diffracted X-ray beams are collimated to a cross section of 0.1 × 0.1 mm to accurately determine unit-cell parameters of the MgO pressure standard. The two-theta angle is fixed at 6° and the intersecting point of the incident and diffracted beams defines a diffracting volume with the longest dimension (about 3 mm) parallel to the incident beam. The imaging apparatus is operated independently from the diffraction components, allowing a quick switchover between diffraction and visual imaging modes during experiments. When entrance slits are removed from the incident beam path, the entire X-ray beam (2 × 1.6 mm cross section) illuminates the sample. In falling-sphere experiments, the absorption contrast caused by the Pt marker sphere is converted into visible light by a single-crystal yttrium/aluminum/garnet (YAG) phosphor on the downstream side of the sample. A mirror reflects the visible contrast into a video camera, and the image is focused by an objective lens.

Assemblies were pressurized while cold, with initial applied loads estimated from previous calibrations of our multianvil assembly (Lesher et al. 2003). Temperature was increased slowly to a temperature ~50 K below the melting point, then increased rapidly at ~800 K per minute to the run temperature. The settling velocity of a Pt sphere was measured in radiographic images of the melt, which were recorded throughout the heating procedure to identify all movement of the sphere in the sample. An example of a falling-sphere experiment is shown as a time series of still images in Figure 2. An energy dispersive X-ray spectrum for the MgO:BN pressure standard was collected immediately following the fall of the marker, and

Table 1. Composition of glass powder used in falling-sphere experiments

	This study	Tinker and Lesher (2001)
SiO_2	67.51 ± 0.58	69.38
TiO_2	0.53 ± 0.04	0.54
Al_2O_3	16.60 ± 0.34	16.87
MgO	3.42 ± 0.06	3.36
CaO	2.89 ± 0.12	3.04
Na_2O	4.09 ± 0.26	3.91
K_2O	4.04 ± 0.16	3.92
NBO/T*	0.1	

Notes: The composition for this study was determined using the Cameca SX-100 electron microprobe at UC Davis. Reported uncertainties are two standard deviations of the mean of 15 measurements. The composition of dacite glass powder used in the Si and O self-diffusion study of Tinker and Lesher (2001) is provided for comparison.

* Following Mysen (1990), we estimated the polymerization index NBO/T from bulk composition as $\mathrm{NBO/T}=1/\mathrm{T}\sum_{i=1}^{i} n\mathrm{M}_i^{n+}$, where NBO is the mole fraction of non-bridging O, T is the mole fraction of tetrahedral cations, and M_i^{n+} is the proportion of network-modifying cation i with electrical charge n+. Network-modifying cations are those remaining after a charge deficiency created when Al^{3+}, Fe^{3+}, or P^{5+} is in tetrahedral coordination has been balanced by allocating K^+, Na^+, Ca^{2+}, Fe^{2+}, and Mg^{2+}, in that order (Mysen 1990).

Table 2. Dacite melt viscosity and parameters used in Stokes' Law

P (GPa)	*T* (K)	Radius × 10^5 (m)*	Velocity × 10^5 (m/s) †	η (Pa·s) ‡
3.8	1730	8.75 ± 0.88	0.62 ± 0.10	39.8 ± 8.0
2.8	1800	4.5 ± 0.5	0.14 ± 0.02	44.1 ± 8.8
3.8	1800	8.75 ± 0.88	1.07 ± 0.16	23.0 ± 4.6
3.8	1800	15 ± 1.5	2.77 ± 0.42	21.5 ± 4.3
4.9	1800	12.5 ± 1.3	5.78 ± 0.87	7.7 ± 1.2
1.5	1825	10 ± 1.0	0.36 ± 0.05	86.6 ± 17.3
3.7	1900	7 ± 0.7	2.28 ± 0.34	7.2 ± 1.4
5	1900	7 ± 0.7	4.32 ± 0.65	3.8 ± 0.8
6.6	1900	9 ± 0.9	9.11 ± 1.37	2.8 ± 0.6
7.1	1950	7.5 ± 0.8	29.1 ± 4.37	0.6 ± 0.1

Notes: The contrast in density between the marker sphere and dacite melt (Δρ) is estimated to be 1.845 ± 0.055 × 10^{-4} kg/m^3 for all experiments. The uncertainty in Δρ is determined using the density of Pt (21.45 g/cm^3) and a melt density of 3 ± 0.5 g/cm^3 (see text).

* 10% uncertainty in sphere radius is based on the resolution of the video monitor and the CCD camera used to record radiographs

† Uncertainty in the settling velocity is estimated to be 15% based on the reproducibility of estimates of terminal velocity (e.g., Fig. 3)

‡ Uncertainty in reported value of viscosity is determined by the propagation of errors in Equation 4. The error contribution from the Faxen correction for wall effects (Eq. 4) comes from the 5% uncertainty in the capsule radius (r_c).

the run pressure was determined using the equation of state (EOS) for MgO.

We estimated pressure (P, in GPa) using a high-temperature formulation of the third-order Birch-Murnaghan equation (e.g., Walter et al. 2002; Utsumi et al. 1998):

$$P = \frac{3}{2}K_{\mathrm{T}}\left[\left(\frac{V_{\mathrm{T}}}{V}\right)^{\frac{7}{3}} - \left(\frac{V_{\mathrm{T}}}{V}\right)^{\frac{5}{3}}\right]\left\{1 - \frac{3}{4}(4 - K_{\mathrm{T}}')\left[\left(\frac{V_{\mathrm{T}}}{V}\right)^{\frac{2}{3}} - 1\right]\right\} \quad (1)$$

where K_{T} (GPa) is the bulk modulus, V_{T} (cm^3/mol) is the unit-cell volume at 1 bar and high temperature, V (cm^3/mol) is the volume at high pressure and high temperature, and K_{T}' is the pressure derivative of the bulk modulus. We estimated V using the positions of major reflections in the energy dispersive MgO X-ray spectrum. The value of K_{T} at high temperature was determined using the relationship:

$$K_{\mathrm{T}} = K_{0,\mathrm{T}} + \left(\frac{\partial K_{\mathrm{T}}}{\partial T}\right)_{\mathrm{P}}(T - 300) \quad (2)$$

where $K_{0,\mathrm{T}}$ is the bulk modulus at 300 K and T is absolute temperature. We used

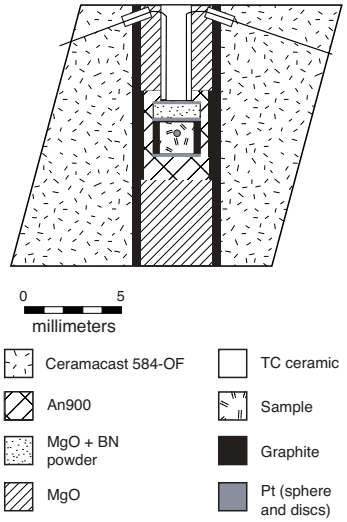

FIGURE 1. Cross section of the multi-anvil assembly used for in situ falling-sphere experiments. A cylindrical sample assembly is inserted into a Ceramacast 584-OF MgO pressure medium. The dacite sample powder is packed inside a graphite cylinder with I.D. of 1.8 mm, and a Pt sphere is placed near the top of the sample. The top and bottom of the capsule are Pt discs. A pressure standard of MgO and BN is placed above the sample.

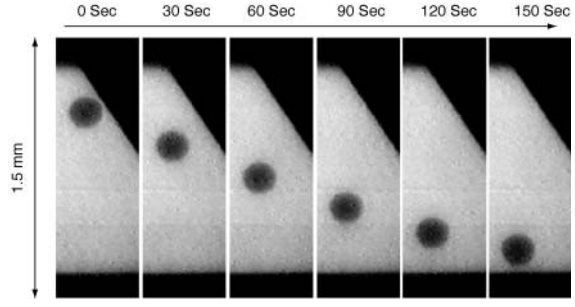

FIGURE 2. Time-lapsed images of a falling sphere experiment. These video images are from an experiment at 3.8 GPa, 1730 K. Time interval between panels is 30 seconds. The Pt sphere (radius of 87.5 μm in this experiment) is clearly visible as a dark shadow against the light grey sample. Dark regions are areas through which X-rays are not transmitted, including Pt discs at the top and bottom of the sample and tungsten carbide anvils in the upper right corner. The viscosity calculated for this experiment is 39.8 ± 8.0 Pa·s.

the results of molecular dynamics (MD) simulations from Matsui et al. (2000) for $K_{0,\mathrm{T}}$ (160.2 GPa), K_{T}' (4.1), and $(\partial K_{\mathrm{T}}/\partial T)_{\mathrm{P}}$ (–0.028 GPa/K). The expression for V_{T} was determined by a third-order least-squares fit to calculated V/V_0 (V_0 = 11.2382 cm^3/mol) at 0 GPa between 300 and 2000 K (Matsui et al. 2000):

$$V_{\mathrm{T}} = 11.14 + 2.885 \times 10^{-4}\,T + 1.498 \times 10^{-7}\,T^2 - 1.736 \times 10^{-11}\,\mathrm{T}^3 \quad (3)$$

The Matsui et al. (2000) values of $K_{0,\mathrm{T}}$ and K_{T}' compare favorably with the results of hydrostatic compression experiments reported by Fei (1999) ($K_{0,\mathrm{T}}$ =160 GPa; K_{T}' = 4.15; $(\partial K_{\mathrm{T}}/\partial T)_{\mathrm{P}}$ = –0.030 GPa/K) and Jackson and Niesler (1982) ($K_{0,\mathrm{T}}$ = 162.5 GPa; K_{T}' = 4.13). However, there is considerable discrepancy between these values and results based on shock compression experiments (e.g., Jamieson et al. 1982, and references therein). For comparison, the Jamieson et al. (1982) data yield pressure estimates for our experiments that are 0.2–0.8 GPa (as much as 20 %) lower than pressures estimated using the approach outlined above. Because the accuracy of equations of state for MgO is debated, we present the volume data for each of our experiments in Table 3.

To determine the settling velocity of falling spheres, videotape recordings of experiments were converted to digital images for computer analysis. The digital images for each experiment were advanced frame-by-frame (each frame is one-thirtieth of a second) and the position of the sphere was determined relative to a measuring grid overlain on the computer screen. The measuring grid was calibrated using known distances in the radiograph image, such as the diameter of the marker sphere at atmospheric pressure. The resolution of the image leads to an uncertainty of 10 μm in distance estimates. Figure 3 shows the time-distance relationship used to determine terminal velocity of the falling sphere (see Table 2 for estimated velocities). Based on the reproducibility of velocity estimates from time-distance relationships, we estimate a 15% uncertainty in terminal velocity. Nonlinear regions at the ends of the time-distance plot in Figure 3 reflect acceleration of the Pt sphere on melting of the sample and deceleration as the sphere approaches the bottom of the sample capsule.

RESULTS

The terminal velocities determined from time-distance relationships have been used to calculate viscosity (η) in a modified form of Stokes' Law:

$$\eta = \frac{2gr^2\Delta\rho}{9v}\left[1 - 2.104\left(\frac{r}{r_{\mathrm{c}}}\right) + 2.09\left(\frac{r}{r_{\mathrm{c}}}\right)^3 - 0.95\left(\frac{r}{r_{\mathrm{c}}}\right)^5\right] \quad (4)$$

where g is the gravitational constant, r is the radius of the falling sphere, Δρ is the density contrast between the sphere and the melt, v is the settling velocity, and r_{c} is the internal radius of the capsule. The term in brackets is the Faxen correction for wall effects on the settling velocity of the sphere (Shaw 1963).

Table 2 shows the values of the variables in Equation 4 and the viscosities calculated for all experiments. The uncertainty reported

TABLE 3. Volume data used to determine run pressures

P (GPa)	Sample T (K)*	V/V_0†	TC T (K)
3.8	1730	1.0350	1710
2.8	1800	1.0470	1783
3.8	1800	1.0385	1773
3.8	1800	1.0385	1773
4.9	1800	1.0300	1773
1.5	1825	1.0600	1823
3.7	1900	1.0445	1873
5	1900	1.0340	1873
6.6	1900	1.0224	1873
7.1‡	1950	1.0012	–

Notes: Calculations of run pressures (see text) are based on the thermocouple (TC) temperature at the time the energy dispersive spectrum of the MgO pressure standard was collected.
* From Table 2.
† V is estimated from major MgO reflections and V_0 = 11.2382 cm^3/mol (Matsui et al. 2000) (see text).
‡ The pressure of this experiment was estimated at 1473 K based on the X-ray spectrum collected before the final heating step, because the thermocouple failed following the fall of the marker sphere.

for these viscosities (±20%) is estimated by propagation of errors in Equation 4 (see Table 2 for a discussion of the uncertainty for each variable in Eq. 4). A potentially important issue is the value of $\Delta\rho$, which is estimated because we have not measured the density of dacite melt at high pressures. As noted by Kushiro (1976), the relative uncertainty in $\Delta\rho$ should be small given the very high density of Pt (21.45 g/cm^3). The density of dacite melt is taken to be 3.0 ± 0.5 g/cm^3, which is within the range of silicate melt densities measured in previous studies (e.g., 2.2–3.5 g/cm^3; Knoche and Luth 1996; Scarfe et al. 1987, and references therein). The large uncertainty accounts for an increase in melt density with pressure, and leads to ~3% uncertainty on $\Delta\rho$.

Figure 4 shows the variation of melt viscosity with pressure at 1800 K and 1900 K. There is a negative pressure dependence on dacite melt viscosity between 2.8 and 4.9 GPa at 1800 K and between 3.7 and 6.6 GPa at 1900 K. For comparison, viscosities measured at 1730 K (3.8 GPa), 1825 K (1.5 GPa), and 1950 K (7.1 GPa) are also illustrated.

The pressure dependence of melt viscosity can be described using the Arrhenius-type relationship:

$$\ln\eta = \ln\eta_0 + \frac{P\Delta V_\eta}{RT} \quad (5)$$

where η_0 is the zero pressure viscosity, P is the pressure in bars, ΔV_η (cm^3/mol) is the activation volume for viscous flow, and R is the gas constant (cm^3·bar/mol·K). Using this approach to quantify the pressure dependence, a negative pressure dependence for melt viscosity is characterized by a negative ΔV_η. The values of $\ln\eta_0$ and ΔV_η in Equation 5 were calculated using a simple linear regression of $\ln\eta$ on P for experiments at 1800 and 1900 K. The errors associated with $\ln\eta_0$ and ΔV_η (Table 4) were estimated using a Monte Carlo approach to the linear regression calculations. The regression coefficients for simple linear regressions were calculated repeatedly, with input parameters (i.e., $\ln\eta$, P, and T) that varied randomly within absolute limits in successive calculations. These absolute limits were ± 0.18 for $\ln\eta$ (equivalent to 20% uncertainty on η), ± 5% for P, and ± 20 K for T. We performed a similar iterative linear regression analysis for previously published viscosity data, using reported uncertainties for $\ln\eta$. The values reported in Table 4 are the mean values of 500 regression calculations, and the uncertainties are one standard deviation of the mean.

The temperature dependence of melt viscosity can be described using the Arrhenius-type relationship:

$$\ln\eta = \ln\eta_0 + \frac{E_\eta}{RT} \quad (6)$$

where η_0 is a pre-exponential factor, E_η is the activation energy for viscous flow, and R (J/mol·K) is the gas constant. The values of $\ln\eta_0$ and E_η in Equation 6 were calculated using simple linear regressions of $\ln\eta$ on $1/T$ for experiments at 3.8 ± 0.1 GPa and 5 ± 0.1 GPa. Errors associated with $\ln\eta_0$ and E_η (Table 5) were estimated using the Monte Carlo approach to the linear regression calculations described for the pressure dependence of viscosity. The absolute limits on input variables in the regressions were ± 0.18 for $\ln\eta$ and ± 20 K for T. The values reported in Table 5 are the mean values of 500 regression calculations, and the uncertainties are one standard deviation of the mean. The calculated activation energies for viscous flow are 275 ± 35 kJ/mol at 3.8 GPa and 210 ± 56 kJ/mol at 5 GPa. These activation energies are similar to the activation energy determined by multiple linear regression for O self-diffusion in dacitic liquid from 1 to 4 GPa (280 kJ/mol, Tinker and Lesher 2001). Using the 5 GPa values for E_η and $\ln\eta_0$ to correct the viscosity at 7.1 GPa from 1950 K to 1900 K, we estimate that dacite melt viscosity is 6.6 Pa·s at 7.1 GPa and 1900 K. This analysis suggests that a minimum viscosity exists between 6.6 and 7.1 GPa. This prediction needs to be confirmed experimentally.

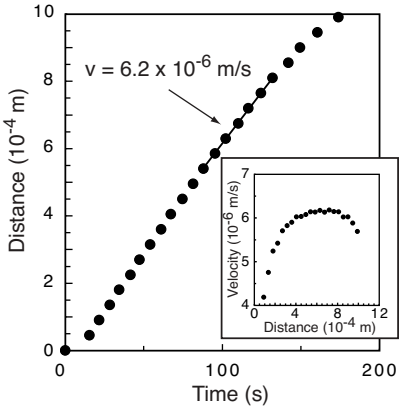

FIGURE 3. Time-distance relationship for a falling-sphere experiment. This plot was used to determine the terminal velocity of the falling sphere in an experiment conducted at 3.8 GPa, 1730 K. The slope of the least-squares, best-fit line through the seven points between 90 and 130 seconds is the velocity used to calculate viscosity for this experiment. The inset shows the velocity-distance relationship for this experiment, with the plateau representing the terminal velocity of the falling sphere.

DISCUSSION

The main result of this study is that dacite melt viscosity decreases with pressure to at least 6.6 GPa. As mentioned earlier,

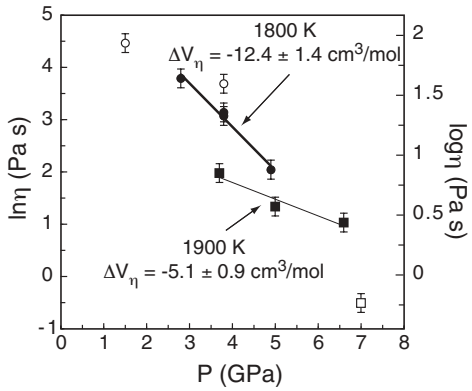

FIGURE 4. Pressure dependence of dacite viscosity. The viscosity of dacite at 1800 K (filled circles) decreases between 2.8 and 4.9 GPa. The viscosity of dacite at 1900 K (filled squares) decreases steadily from 3.7 to 6.6 GPa. For comparison, viscosities measured in experiments at 1825 K (1.5 GPa), 1730 K (3.8 GPa), and 1950 K are also shown (open circles). The activation volumes for viscous flow at 1800 and 1900 K were calculated using Equation 2 (see text). Error bars show ±20% uncertainty for all experiments. Lines through data are least squares best fits to data from 1800 K and 1900 K.

TABLE 4. Activation volume for viscous flow (ΔV_η) and activation volume for O self-diffusion (ΔV_a) for dacite, albite, and diopside melt compositions

Coefficients for simple linear regression

Viscous flow

	Dacite (this study)		Albite		Diopside	
T (K)	ΔV_η (cm³/mol)	$\ln\eta_0$	ΔV_η (cm³/mol)	$\ln\eta_0$	ΔV_η (cm³/mol)	$\ln\eta_0$
1673			–15.0(9)*	9.6(1)*		
1800	–12.4(14)	6.2(4)				
1873			–16.0(18)†	6.5(1)†	18.8(21)‡	–1.9(1)‡
			–4.5(2)§	3.62(5)§		
1900	–5.1(9)	3.1(3)				
1973			–5.3(1)#	2.67(2)#		
2000			–10.5(7)**	3.4(2)**		

O self-diffusion

	Dacite††		Albite	Diopside	
T (K)	ΔV_a (cm³/mol)	$\ln D_0$	ΔV_a (cm³/mol)	ΔV_a (cm³/mol)	$\ln D_0$
1733	–14.5(13)	–30.6(2)			
1834	–9.8(10)	–28.6(1)			
1923				8.48(13)‡‡	
1935	–8.8(18)	–27.7(1)			
2100			–8.3§§		
2273				2.7(4)***	–20.3(1)***

Coefficients for multiple linear regression (O self-diffusion) †††

	ΔV_n (cm³/mol)	E_n (kJ/mol)	$\ln D_0$
Dacite	–11.1(7)	280(12)	–10.6(8)

Notes: Errors in parentheses are given in terms of the least unit cited, e.g., –12.4(14) represents –12.4 ± 1.4 and 8.48(13) represents 8.48 ± 0.13.
* Calculated using data from 0.5 to 2 GPa (Kushiro 1978).
† Calculated using data for 1 atm to 1.5 GPa (Brearley et al. 1986).
‡ Calculated for 0.5 to 1.5 GPa (from Brearley et al. 1986).
§ Calculated from Suzuki et al. (2002) (3.3–4.6 GPa).
# Calculated from Suzuki et al. (2002) (2.6–5.3 GPa).
** Calculated using data from Mori et al. (2000) (3–7 GPa).
†† Tinker and Lesher (2001) (1–4 GPa).
‡‡ Shimizu and Kushiro (1984) (1–1.7 GPa).
§§ Poe et al. (1997) (2.5–4 GPa).
*** Calculated using data from 3 to 6 GPa (Reid et al. 2001).
††† Results of regressions for the combined P and T effect on D(O) from 1 to 4 GPa and 1733 to 1935 K (Tinker and Lesher 2001).

TABLE 5. Activation energies (E_η) for viscous flow of dacite melt

P (GPa)*	E_η (kJ/mol)	$\ln\eta_0$
3.8	275 ± 35	–15.3 ± 2.3
5	210 ± 56	–12.0 ± 3.7

* The regressions include experiments at the pressures listed here, and experiments at pressures within 0.1 GPa of these pressures.

a decrease in viscosity with pressure was also observed in studies of fully polymerized jadeite (Kushiro 1976) and albite (Suzuki et al. 2002; Mori et al. 2000; Kushiro et al. 1978) melts. These studies supported two models to explain the negative pressure dependence of viscosity. Mori et al. (2000) suggested that viscous flow in albite melt is enhanced on compression by weakening of the T-O bond (T is a tetrahedral cation such as Si or Al) due to shortening of the T-O bond and a decrease of the T-O-T bond angle. In contrast, Kushiro (1976) proposed that the formation of high-coordinated Al caused the negative pressure dependence of the viscosity of fully polymerized jadeite melt. Suzuki et al. (2002) invoked this latter mechanism for viscous flow in albite, and based on MD simulations predicted that the populations of five- and six-coordinated Si and Al in albite melt steadily increase with pressure to at least 6 GPa.

Viscous flow could be facilitated by five-coordinated Si or Al species, which form when a non-bridging O bonds to a nearby tetrahedron. If the five-coordinated species is then separated from one of its original O neighbors, a change in local melt structure results and viscous flow has occurred (Liu et al. 1988). This process could increase the rate of viscous flow at high pressures where the abundance of high-coordinated species increases (e.g., Yarger et al. 1995).

Interestingly, recent studies of Si and O self-diffusion in polymerized melts have also adopted the mechanism involving five-coordinated Si and Al species (e.g., Lesher et al. 1996; Poe et al. 1997; Tinker and Lesher 2001). If the same mechanism controls viscous flow and Si and O self-diffusion in polymerized melts, we might expect similarities in the pressure dependence for these melt transport properties. In the following discussion, we investigate the relationship between O self-diffusion and melt viscosity using our new data on dacite melt viscosity, available data on albite melt viscosity (Kushiro et al. 1978; Mori et al. 2000; Suzuki et al. 2002), and O self-diffusion coefficients in dacite (Tinker and Lesher 2001) and albite (Poe et al. 1997) melts.

The Eyring relationship

The negative pressure dependence of dacite melt viscosity is predicted by O self-diffusion coefficients [D(O)] in dacite melt, which show an increase with pressure between 1 and 4 GPa (Tinker and Lesher 2001). The inverse relationship between D(O) and melt viscosity can be described by the Eyring equation:

$$\eta = \frac{k_B T}{D(O)\lambda} \quad (7)$$

where k_B is the Boltzmann constant and λ is the jump distance for self-diffusion. A critical assumption in Equation 7 (with λ = 2.8 Å, the diameter of the O^{2-} anion) is that viscous flow is accommodated by the activation of the O^{2-} anion.

The Eyring equation (with λ = 2.8 Å) has been used successfully to estimate the viscosities of a few polymerized melts at high pressures. Shimizu and Kushiro (1984) reported O self-diffusion in jadeite melt from 0.5 to 2 GPa, and showed that the Eyring relationship (with λ = 2.8 Å) accurately reproduced measured viscosities. Rubie et al. (1993) used the Eyring equation to estimate the viscosities of $Na_2Si_4O_9$ melt between 2.5 and 10 GPa, and extrapolated these viscosities to low pressure. Their viscosities for low pressure agreed with the temperature-corrected viscosity of $Na_2Si_4O_9$ at 1 atm. Similarly, Poe et al. (1997) predicted viscosities of albite melt between 2.5 and 6 GPa at 2100 K, and found that extrapolations to low pressures were consistent with temperature-corrected viscosities measured between 1 atm and 2 GPa (Kushiro 1978). It is interesting that the Eyring equation is found to successfully predict the viscosities of jadeite melt, in which O self-diffusion is proposed to occur by the activation of O^{2-} anions (Shimizu and Kushiro 1984), as well as the viscosities of $Na_2Si_4O_9$ and albite melts in which O self-diffusion has been described by a model involving high-coordinated species (Rubie et al. 1993; Poe et al. 1997).

In contrast, the Eyring equation (with λ = 2.8 Å) does not successfully predict the viscosities of depolymerized melts. Shimizu and Kushiro (1984) found that the Eyring equation did not accurately predict the viscosity of diopside melt between 1 and 1.7 GPa, while Reid et al. (2001) demonstrated this at higher pressures. Dunn (1982) found good agreement between O self-diffusion coefficients and melt viscosities for diopside, $Di_{58}An_{42}$,

and $Di_{40}An_{60}$ melt compositions when jump distances greater than 2.8 Å were assumed. He concluded that diffusion and viscous flow for these melts involve the activation of larger, molecular species [i.e., $(SiO_4)^{4-}$] rather than individual ions.

To evaluate the Eyring equation for a naturally occurring silicate melt, we used the results of this study and our data for O self-diffusion (Tinker and Lesher 2001). Figure 5 directly compares our measured viscosities of dacite melt with viscosities recovered from the Eyring equation assuming $\lambda = 2.8$ Å and D(O) derived from Tinker and Lesher (2001) at identical pressure and temperature. This comparison shows that the Eyring equation overestimates viscosity for all but our highest pressure (>5 GPa), lowest viscosity results. The agreement between measured and predicted viscosities is generally improved if the translation distance (λ) in the Eyring equation is increased to 3.6–5.3 Å.

The overestimates of viscosity in Figure 5 can be related to the mechanisms for O self-diffusion in dacite melt. For example, at 1733 K, the absolute magnitudes of the activation volumes for Si and O self-diffusion (ΔV_a,14.5–17.1 cm^3/mol) are much greater than the molar volume of O (6.9 cm^3/mol). These differences are consistent with the transport of Si and O as a molecular species, such as SiO_2. However, at 1834 and 1935 K, the absolute magnitudes of activation volumes for Si and O self-diffusion (8.7–9.8 cm^3/mol) approach the molar volume of O. We suggest that diffusion at these temperatures occurs through a combination of mechanisms, which may include ionic diffusion, but largely involves the formation and disassociation of five-coordinated Si and Al species (Tinker and Lesher 2001; Poe et al. 1997; Rubie et al. 1993). As noted above, we found that agreement between measured and predicted viscosity improves for the higher pressure and temperature conditions. This observation for dacite suggests that predictions of the Eyring equation will improve as the magnitude of ΔV_a nears the molar volume of O, consistent with previous use of the Eyring equation when O self-diffusion is ionic (e.g., Shimizu and Kushiro 1984) and when O self-diffusion occurs through the formation of five-coordinated Si or Al (Rubie et al. 1993; Poe et al. 1997). Although the latter mechanism is more complicated than the simple jumping model commonly assumed by the Eyring equation, the net volume change associated with transient formation of high-coordinated species is small and of the same order as the molar volume of O.

Alternatively, the success of the Eyring equation may depend on the similarity of the magnitudes of activation volumes for self-diffusion and viscous flow (ΔV_η). Figure 5 shows that the Eyring equation overestimates dacite viscosity at both 1800 K and 1900 K, although the magnitude of ΔV_η at 1900 K is much closer to the molar volume of O (see Table 4 for a comparison of ΔV_a and ΔV_η). The above discussion suggests that accurate predictions of melt viscosity using the Eyring equation may be fortuitous.

A more complete understanding of viscous flow, and of the relationship between self-diffusion and viscosity, will likely come from Adam-Gibbs theory (Adam and Gibbs 1965). The Adam-Gibbs description of structural relaxation has been used to infer the number of Si-O tetrahedra involved in viscous flow of sodium silicate liquids (Toplis 2001), and modified Adam-Gibbs theory has been adapted to explain the pressure dependence of viscosity (Bottinga and Richet 1995) and self-diffusion (Tinker et al. 2003). Recently, Mungall (2002) used Adam-Gibbs theory to develop empirical models to relate viscosity and self-diffusion, and showed that the two processes can be decoupled if O self-diffusion does not require the rearrangement of melt structure.

Sign of the pressure dependence and viscosity minima

In our study of Si and O self-diffusion in dacite melt (Tinker and Lesher 2001), we found that both Si and O self-diffusion coefficients reach maximum values at 5 GPa. Similarly, Poe et al. (1997) reported maximum O self-diffusion coefficients in albite (5 GPa) and $Na_3AlSi_7O_{17}$ (8 GPa) melt compositions. These self-diffusivity maxima are thought to coincide with maximum populations of five-coordinated Si or Al. One consequence of a decrease in the population of five-coordinated Si and Al will be a reduction in the availability of O to form high-coordinated species. This expectation is supported by spectroscopic evidence that the population of five-coordinated Al in $Na_3AlSi_7O_{17}$ melt reaches a maximum at 8 GPa (Yarger et al. 1995). If self-diffusion and viscous flow occur by the same mechanism, viscous flow also should be affected by the proportion of five-coordinated species. The viscosity of dacite, albite, and $Na_3AlSi_7O_{17}$ compositions should pass through minima at high pressure.

Measurements of the viscosity of dacite and albite show no conclusive evidence of a minimum at high pressures (Fig. 6). Figure 6a compares dacite viscosity measured in this study with viscosities predicted by the Eyring equation with D(O) measured at 1935 K (Tinker and Lesher 2001). Because we have shown that D(O) reaches a maximum at 5 GPa, the Eyring equation predicts a minimum in viscosity at that pressure. Our new direct measurements of viscosity under similar pressures and temperatures do not indicate that a viscosity minimum exists at 5 GPa, but rather that viscosity continues to drop with increasing pressure to at

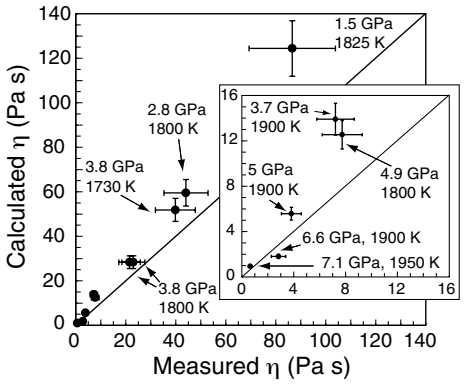

FIGURE 5. Comparison of measured and calculated viscosities of dacite. Viscosities measured in this study are plotted on the abscissa, and calculated viscosities are plotted on the ordinate. The calculated viscosities were determined using the Eyring equation with a jump distance λ = 2.8 Å. The O self-diffusion coefficients used in the Eyring equation were estimated for run conditions of this study using the relationship $\ln D(O) = \ln D_0 - (E_a + P\Delta V_a)/RT$, with $\ln D_0$ (–10.6 ± 0.8), E_a (280 ± 12 kJ/mol), and ΔV_a (–11.1 ± 0.7 cm^3/mol) from Tinker and Lesher (2001). Note that for most experimental conditions, the Eyring equation estimates viscosities that are greater than measured viscosities. The inset provides details of the low-viscosity region of the plot. Error bars show ± 20% uncertainties on measured viscosity and ±10% uncertainty on calculated viscosity.

least 6.6 GPa. It is anticipated that the viscosity of dacite melt will reach a minimum value at higher pressure, however, this expectation will need to be evaluated by further study.

Figure 6b compares albite melt viscosities predicted by the Eyring equation with viscosities of the same composition measured directly at high pressure. Poe et al. (1997) predicted a minimum viscosity near 5 GPa, based on a maximum in O self-diffusion coefficients at that pressure. However, recent viscosity measurements have not confirmed the existence of this viscosity minimum. Mori et al. (2000) found a decrease in the viscosity of albite melt between 3 and 7 GPa at 2000 K. Although there is an apparent minimum viscosity between 5 and 6 GPa, Mori et al. stated that this change in slope may be an artifact of the large uncertainty associated with their fall-and-quench experiments. Suzuki et al. (2002) conducted in situ falling-sphere viscometry experiments and reported that albite viscosity continues to decrease with pressure to at least 5.3 GPa.

The measured viscosities of dacite and albite in Figure 6 are not predicted accurately by O self-diffusion coefficients at the same pressures. If a minimum viscosity exists at higher pressures, the current data sets suggest that O self-diffusion coefficients pass through maxima at pressures different from pressures at which melt viscosities pass through minima. The existence of a minimum in viscosity and a maximum diffusivity at different pressures may indicate that the nature of the structural rearrangement required for the transport of O by diffusion is different from that permitting melts to deform by shear flow. A continued comparison between dacite and albite is critical to understanding compositional controls on the transport properties of naturally occurring melts. Differences in the pressure dependence of dacite and albite viscosities could be attributed to additional network-modifiers in dacite weakening network bonds or influencing order/disorder of network formers (particularly five-coordinated Si and Al).

CONCLUDING REMARKS

We have shown that dacite melt viscosity has a negative pressure dependence to at least 6.6 GPa. In general, this negative pressure dependence suggests that the mobility of relatively polymerized melts such as basalts or more silicic compositions will be enhanced at high pressures in the Earth's mantle. Baker et al. (1995) found silica-rich (~57 wt% SiO_2), low-degree partial melts of peridotite in experiments at 1 GPa and 1523 K. These authors noted that the calculated viscosity of one low-degree, silicic melt (~200 Pa·s) was much greater than the viscosities of 0.1-10 Pa·s typically used in models of melt behavior in the mantle (Baker et al. 1995, and references therein). The viscosity of dacite melt we measure at 1.5 GPa and 1825 K (86.6 Pa·s) is generally consistent with the Baker et al. (1995) estimate, and is likely to be more viscous at lower pressure and temperature. Such high-viscosity partial melts will not segregate readily from residual solids in the shallow mantle, and should be considered in models of melt extraction.

The negative pressure dependence of dacite melt to 6.6 GPa is surprising, because O self-diffusion coefficients in dacite melt reach a maximum value at 5 GPa and the Eyring equation predicts a minimum in melt viscosity at this pressure (Tinker and Lesher 2001). This result is critical because previous studies have estimated melt viscosity indirectly (e.g., Poe et al. 1997), assuming that the pressure dependences of melt viscosity and self-diffusion will always have different signs. The possibility that self-diffusion and viscosity respond differently to compression emphasizes the need for direct measurements of both transport properties at pressures greater than 7 GPa. Such studies could confirm differences in pressure dependence of self-diffusion and melt viscosity in polymerized compositions. One explanation for a difference in the pressure dependence is that different mechanisms control self-diffusion and viscous flow. Earlier, we advocated the formation of high-coordinated species for Si and O self-diffusion in dacite melt, and speculated that maximum self-diffusion coefficients coincided with maximum populations of five-coordinated

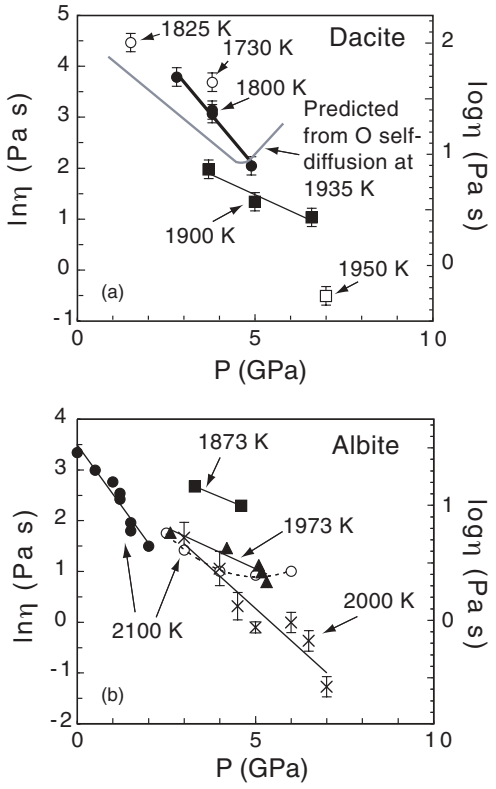

FIGURE 6. Pressure dependence of viscosity for dacite and albite melts. (**a**) Comparison of measured dacite viscosity with viscosity predicted using Eyring equation. The pressure dependence for measured viscosities at 1800 K (filled circles) and 1900 K (filled squares) are shown by least-squares, best-fit lines to these data. Additional data points are viscosities measured at 1825 K, 1.5 GPa, 1730 K, 3.8 GPa (open circles), and 7.1 GPa, 1950 K (open square). The grey curve shows the pressure dependence of viscosity predicted using the Eyring equation with O self-diffusion coefficients measured at 1935 K (Tinker and Lesher 2001). The predicted pressure dependence changes sign at 5 GPa, but the measured viscosities do not show this minimum in viscosity. (**b**) Viscosity of albite. The open circles are viscosities predicted at 2100 K by Poe et al. (1997) using the Eyring equation with measured O self-diffusion coefficients. The dashed line through these data is a second-order polynomial fit. Filled circles are viscosities measured by Kushiro (1978) and adjusted to 2100 K by Poe et al. (1997) (see text). Other measurements shown are from Suzuki et al. (2002) at 1873 K (squares) and 1973 K (triangles), and from Mori et al. (2000) at 2000 K (X symbols). The pressure dependence of measured viscosities does not show the change in sign predicted by O self-diffusion.

Si and Al (Tinker and Lesher 2001). Although the mechanism for viscous flow appears insensitive to the saturation of the melt with five-coordinated species, it may be related to the distribution of these species in the melt. In a recent nuclear magnetic resonance study, Lee et al. (2003) found an increase with pressure in the ordering of five- and six-coordinated Si in sodium silicate glass. The degree of disorder of high-coordinated species in the melt will change the configurational entropy of a melt, and thereby affect melt viscosity as described by Adam-Gibbs theory (Adam and Gibbs 1965; Bottinga and Richet 1995). Future experimental studies of melt transport properties at high pressures may provide constraints necessary to build on promising formulations of the Adam-Gibbs theory to relate self-diffusion and melt viscosity.

ACKNOWLEDGMENTS

The authors thank B.O. Mysen and an anonymous reviewer for comments that improved the manuscript. The authors also acknowledge D.B. Dingwell for editorial handling and M. Walter for discussions concerning the EOS of MgO. This work was supported by grants NSF EAR00-01245 and UC CARE (03-04) to C.E.L. This work was performed at GeoSoilEnviroCARS (GSECARS), at the Advanced Photon Source, Argonne National Laboratory, and the authors acknowledge the GSECARS staff for technical and scientific support. Use of the Advanced Photon Source was supported by the U.S. Department of Energy, Office of Science, Office of Basic Energy Sciences, under contract no. W-31-109-ENG-38.

REFERENCES CITED

Adam, G. and Gibbs, J.H. (1965) On the temperature dependence of cooperative relaxation properties in glass-forming liquids. Journal of Chemical Physics, 43, 139–146.

Baker, M.B., Hirschmann, M.M., Ghiorso, M.S., and Stolper, E.M. (1995) Compositions of near-solidus peridotite melts from experiments and thermodynamic calculations. Science, 375, 308–311.

Bottinga, Y. and Richet, P. (1995) Silicate melts: The "anomalous" pressure dependence of the viscosity. Geochimica et Cosmochimica Acta, 59, 2725–2731.

Brearley, M., Dickinson, J.E., Jr., and Scarfe, C.M. (1986) Pressure dependence of melt viscosities on the join diopside-albite. Geochimica et Cosmochimica Acta, 50, 2563–2570.

Dunn, T. (1982) Oxygen diffusion in three silicate melts along the join diopside-anorthite. Geochimica et Cosmochimica Acta, 46, 2293–2299.

Fei, Y. (1999) Effects of temperature and composition on the bulk modulus of (Mg,Fe)O. American Mineralogist, 84, 272–276.

Hazen, R.M. and Sharpe, M.R. (1983) Radiographic determination of the position of platinum spheres in density-viscosity studies of silicate melts. Carnegie Institute of Washington Yearbook, 82, 428–430.

Jackson, I. and Niesler, H. (1982) The elasticity of periclase to 3 GPa and some geophysical implications. In Akimoto, S. and Manghnani, M.H., Eds., High Pressure Research in Geophysics, 93–113. D. Reidel Publishing Company, Boston.

Jamieson, J.C., Fritz, J.N., and Manghnani, M.H. (1982) Pressure measurement at high temperature in X-ray diffraction studies: Gold as a primary standard. In Akimoto, S. and Manghnani, M.H., Eds., High Pressure Research in Geophysics, p. 27–48. D. Reidel Publishing Company, Boston.

Kanzaki, M., Kurita, K., Fujii, T., Kato, T., Shimomura, O., and Akimoto, S. (1987) A new technique to measure the viscosity and density of silicate melts at high pressure. In Manghnani, M.H. and Syono, Y., Eds., High Pressure Research in Mineral Physics, p. 195–200. American Geophysical Union, Washington, D.C.

Knoche, R. and Luth, R.W. (1996) Density measurements on melts at high pressure using sink/float method: Limitations and possibilities. Chemical Geology, 128, 229–243.

Kushiro, I. (1976) Changes in viscosity and structure of melt of $NaAlSi_2O_6$ composition at high pressures. Journal of Geophysical Research, 81, 6347–6350.

——— (1978) Viscosity and structural changes of albite ($NaAlSi_3O_8$) melt at high pressures. Earth and Planetary Science Letters, 41, 87–90.

Lee, S.K., Fei, Y., Cody, G.D., and Mysen, B.O. (2003) Order and disorder in sodium silicate glass and melts at 10 GPa. Geophysical Research Letters, 30, 1845.

Lesher, C.E., Hervig, R.L., and Tinker, D. (1996) Self-diffusion of network formers (silicon and oxygen) in naturally occurring basaltic liquid. Geochimica et Cosmochimica Acta, 60, 405–413.

Lesher, C.E., Pickering-Witter, J., Baxter, G., and Walter, M. (2003) Melting of garnet peridotite: Effects of capsules and thermocouples, and implications for the high-pressure mantle solidus. American Mineralogist, 88, 1181–1189.

Liu, S.-B., Stebbins, J.F., Schneider, E., and Pines, A. (1988) Diffusive motion in alkali silicate melts: an NMR study at high temperature. Geochimica et Cosmochimica Acta, 58, 3653–3664.

Matsui, M., Parker, S.C., and Leslie, M. (2000) The MD simulation of the equation of state of MgO: Application as a pressure calibration standard at high temperature and pressure. American Mineralogist, 85, 312–316.

Mori, S., Ohtani, E., and Suzuki, A. (2000) Viscosity of the albite melt to 7 GPa at 2000 K. Earth and Planetary Science Letters, 175, 87–92.

Mungall, J.E. (2002) Empirical models relating viscosity and tracer diffusion in magmatic silicate melts. Geochimica et Cosmochimica Acta, 66, 125–143.

Mysen, B.O. (1990) Relationships between silicate melt structure and petrologic processes. Earth Science Reviews, 27, 281–365.

Poe, B.T., McMillan, P.F., Rubie, D.C., Chakraborty, S., Yarger, J., and Diefenbacher, J. (1997) Silicon and oxygen self-diffusivities in silicate liquids measured to 15 gigapascals and 2800 Kelvin. Science, 276, 1245–1248.

Reid, J.E., Poe, B.T., Rubie, D.C., Zotov, N., and Wiedenbeck, M. (2001) The self-diffusion of silicon and oxygen in diopside ($CaMgSi_2O_6$) liquid up to 15 GPa. Chemical Geology, 174, 77–86.

Reid, J.E., Suzuki, A., Funakoshi, K., Terasaki, H., Poe, B.T., Rubie, D.C., and Ohtani, E. (2003) The viscosity of $CaMgSi_2O_6$ liquid at pressures up to 13 GPa. Physics of the Earth and Planetary Interiors, 139, 45–54.

Rivers, M.L., Duffy, T.S., Wang, Y., Eng, P.J., Sutton, S.R., and Shen, G. (1998) A new facility for high-pressure research at the advanced photon source. In Manghnani, M.H. and Yagi, T., eds.: Properties of Earth and Planetary Materials at High Pressure and Temperature, p. 79–87 Geophysical Monograph 101, American Geophysical Union, Washington, D.C.

Rubie, D.C., Ross, C.R. II, Carroll, M.R., and Elphick, S.C. (1993) Oxygen self-diffusion in $Na_2Si_4O_9$ liquid up to 10 GPa and estimation of high-pressure melt viscosities. American Mineralogist, 78, 574–582.

Rutter, M.D., Secco, R.A., Liu, H., Uchida, T., Rivers, M.L., Sutton, S.R., and Wang, Y. (2002), Viscosity of liquid Fe at high pressure, Physical Reviews (B), 66, 060102–2–060102–4.

Scarfe, C.M., Mysen, B.O., and Virgo, D. (1987) Pressure dependence of the viscosity of silicate melts. In Mysen, B.O., Ed., Magmatic Processes: Physicochemical Principles, p. 59–67 Special Publication No.1, The Geochemical Society. University Park, PA.

Secco, R.A., Rutter, M.D., Balog, S.P., Liu, H., Rubie, D.C., Uchida, T., Frost, D., Wang, Y., Rivers, M.L., and Sutton, S.R. (2002) Viscosity and density of Fe-S liquids at high pressures. Journal of Physics: Condensed Matter, 14, 11325–11330.

Shaw, H.R. (1963) Obsidian-H_2O viscosities at 1000 and 2000 bars in the temperature range 700° to 900° C. Journal of Geophysical Research, 68, 6337–6343.

Shimizu, N. and Kushiro, I. (1984) Diffusivity of oxygen in jadeite and diopside melts at high pressures. Geochimica et Cosmochimica Acta, 48, 1295–1303.

Suzuki, A., Ohtani, E., Funakoshi, K., Terasaki, H., and Kubo, T. (2002) Viscosity of albite melt at high pressure and high temperature. Physics and Chemistry of Minerals, 29, 159–165.

Tinker, D. and Lesher, C.E. (2001) Self-diffusion of Si and O in dacitic liquid at high pressures. American Mineralogist, 86, 1–13.

Tinker, D., Lesher, C.E., and Hutcheon, I.D. (2003) Self-diffusion of Si and O in diopside-anorthite melt at high pressures. Geochimica et Cosmochimica Acta, 67, 133–142.

Toplis, M.J. (2001) Quantitative links between microscopic properties and viscosity of liquids in the system SiO_2-Na_2O. Chemical Geology, 174, 321–331.

Uchida, T., Wang, Y., Rivers, M.L., and Sutton, S.R. (2001) Stability field and thermal equation of state of ε-iron determined by synchrotron x-ray diffraction in a multianvil apparatus. Journal of Geophysical Research, 106, 21799–21810.

Uchida, T., Wang, Y., Rivers, M.L., Sutton, S.R., Weidner, D.J., Vaughan, M.T., Chen, J., Li, B., Secco, R.A., Rutter, M.D., and Liu, H. (2002) A large-volume press facility at the Advanced Photon Source: Diffraction and imaging studies on materials relevant to the cores of planetary bodies. Journal of Physics: Condensed Matter, 14, 11517–11523.

Utsumi, W., Weidner, D.J., and Liebermann, R.C. (1998) Volume measurement of MgO at high pressures and high temperatures. In Manghnani, M.H. and Yagi, T., Eds., Properties of Earth and Planetary Materials at High Pressure and Temperature, p. 327–333. Geophysical Monograph 101, American Geophysical Union, Washington, D.C.

Walker, D. (1991) Lubrication, gasketing, and precision in multianvil experiments. American Mineralogist, 76, 1092–1100.

Walter, M., Katsura, T., Kubo, A., Shinmei, T., Nishikawa, O., Ito, E., Lesher, C., and Funakoshi, K. (2002) Spinel-garnet lherzolite transition in the system CaO-MgO-Al_2O_3-SiO_2 revisited: An in situ X-ray study. Geochimica et Cosmochimica Acta, 66, 2109–2121.

Yarger, J.L., Smith, K.H., Nieman, R.A., Diefenbacher, J., Wolf, G.H., Poe, B.T., and McMillan, P.F. (1995) Al coordination changes in high-pressure aluminosilicate liquids. Science, 270, 1964–1967.

MANUSCRIPT RECEIVED DECEMBER 10, 2003
MANUSCRIPT ACCEPTED JULY 20, 2004
MANUSCRIPT HANDLED BY DONALD DINGWELL